Black Sea Journal of Engineering and Science
doi: 10.34248/bsengineering.1239298

Open Access Journal
e-ISSN: 2619 – 8991

Research Article
Volume 6 - Issue 2: 60-67 / April 2023

DETERMINING ACCURACY OF TEMPERATURE LIMIT CHANGE IN POWER TRANSFORMER CORE USING TEMPERATURE-TIME PARAMETER METHOD

Nihat PAMUK[1]*

[1]*Zonguldak Bulent Ecevit University, Faculty of Engineering, Department of Electrical Electronics Engineering, 67100, Zonguldak, Türkiye*

Abstract: The efficient transmission of electrical energy depends on amplifying voltage values with power transformers. To obtain higher efficiency from transformers, the core and winding type of transformer, the geometric structure of the core, and the shaping techniques in the windings are changed. This requires modeling transformer windings with equivalent circuits and calculating the inductance and electrical parameters appropriately. In this study, two-dimensional (2D) finite element solutions with energy perturbation and flux-coupling methods are used. The correctness of the inductance values of transformer windings was established, and the design was performed, by considering the inductance and electrical parameter values, which are comparable to the energy perturbation and flux connection. However, when two-dimensional calculated fields are used, the flux coupling method requires less computation and gives numerically more accurate results than the energy perturbation method. So, it is concluded that the flux-coupling approach should be chosen as the preferred method for calculating the inductance and electrical parameters of transformer windings. The numerical properties and equivalence of energy perturbation and flux-connection methods, the "apparent" inductance value of the primary and secondary field windings of power transformer operating under transient conditions, using the temperature-time parameter method, are calculated and its accuracy is demonstrated.

Keywords: Power transformer windings, Energy perturbation method, Flux-linkage method, 2D finite element methods, Transient condition

***Corresponding author:** Zonguldak Bulent Ecevit University, Faculty of Engineering, Department of Electrical Electronics Engineering, 67100, Zonguldak, Türkiye
E mail: nihatpamuk@gmail.com (N. PAMUK)
Nihat PAMUK https://orcid.org/0000-0001-8980-6913

Received: January 19, 2023
Accepted: February 23, 2023
Published: April 01, 2023

Cite as: Pamuk N. 2023. Determining accuracy of temperature limit change in power transformer core using temperature-time parameter method. BSJ Eng Sci, 6(2): 60-67.

1. Introduction

The electrical transmission and distribution system includes power transformers as a critical component. Losses in power transformers are become more significant due to rising energy costs (Metwally, 2011). The increase in the use of electronic elements causes the formation of current harmonics in the system (Delghavi et al., 2021). This increases the losses in power transformers. If the losses in the power transformers are not kept under control, it causes the temperature in the power transformer core to increase and the insulation deteriorates (Pamuk, 2017; Mariprasath and Ravindaran, 2022). Load losses in power transformers are examined in three main sections. These are DC losses, eddy current losses in the windings, and leakage losses occurring in the tank and other conductive parts of the power transformer (Ertl and Landes, 2007). The values of DC loss are the simplest to compute and quantify. Eddy current losses in the power transformer's winding and other components cannot be detected during the measurement. These values can only be estimated by computation or modeling in two-dimensional finite element programs (Kwon and Bang, 2018). It has been successful to estimate the performance of temperature-time parameters for electrical power transformer equipment in steady-state using 2D finite element techniques (2D-FETs) (Mejia-Barron et al., 2018), (Shadab et al., 2023) and transient (Oliveira et al., 2012; Božidar et al., 2017) conditions. Nevertheless, the electrical power transformer model obtained with lots of variables is far too detailed for many applications, such as power system analysis, and therefore, it is common practice to seek comparable circuit simulations with resistances and inductors obtained from finite element solutions.

Numerical inductance estimation of physically realizable equipment windings, such as the main and secondary field core of electrical power transformers, comprises the post-processing of nonlinear finite element solutions. The energy perturbation (EP) method (He, 2003), and the reputable flux-linkage (FL) approach have both been used for this purpose (Fornasiero et al., 2014). The first involves using the right permeability values from the numerical model to calculate co-energies around the electrical device under consideration's operating point. The FL method consists of calculating flux linkages created by specific currents. Both approaches yield equivalent inductance values. The EP approach is laborious and may be numerically unstable because it includes the variance among values of identical size (Johnson et al., 2014), and to get precise solutions, current perturbations must be properly selected. Furthermore, because area integrations are required, computational expenses are extremely substantial. On the other hand, when 2D numerically determined fields are used, the FL approach is simpler to use and has reduced computing costs.

A power transformer's load capacity and useful life limit values must be estimated, as well as the hot spot limit values of the power transformer core windings. Many methods have been proposed to determine the hot spot limit values under sinusoidal conditions (Kunicki et al., 2020; Emiroglu et al., 2021). This paper proposes a heat transfer theory-based thermal modeling approach for equivalent circuit transformers. The degradation time of the insulation level in transformer windings is evaluated using full simulation and iterative process methodologies. The transformer's design stage and the likelihood that it will fail within a certain time period affect how long it will operate efficiently (Awadallah et al., 2014). Many analytical methods have been developed to estimate the temperature values and distributions at different points of the transformer windings. These methods are closed-form methods using the generalized heat conduction model and are based on mathematical techniques (Lee et al., 2010; Ding and Ning, 2012). However, some methods can evaluate the hot spot distribution in transformer windings under harmonic conditions. To estimate the hot spot distribution and lifetime in power transformers, structures similar to the conventional transformer equivalent circuit model should be used.

2. Calculation of Diverse Inductance Losses

The energy stored in power transformer windings is directly measured by the inductance (Hashemnia et al., 2015). It also serves as an opposite measurement of the current generated in a winding. As a result, precise inductance value calculation is required to represent electrical power transformers with similar circuits. There are several definitions of inductance (Oliveira, 2014). However, calculations for electrical power transformer windings frequently use the apparent and differential values. Due to the notation difference, the differential is utilized in this instance instead of incremental. The ultimate current and flux values determine the apparent inductance. The straight line that connects the origin and the operational point on the nonlinear magnetizing characteristic serves as its representation. The slope of the nonlinear curve at the operational point determines the differential inductance.

2.1. Method for Calculating Apparent Inductance Losses Numerically

The EP method or the FL approach can be used to determine the apparent inductance for linearized equipment. It is important to use the magnetic co-energy that can be proved for a multi-winding system in order to employ the complicated procedure that is used to determine the apparent values of current perturbations and inductance equation 1 (Shirakawa et al., 2016);

$$dW_{stored} = i.d\lambda = e.idt \tag{1}$$

where e is the voltage, i is the current, and λ is the flux linkage. The relationship between i - λ is non-linear. If there is a finite change in flux connection from one value to another, (λ_1 to λ_2) it can be calculated as equations 2-6:

$$\Delta W_{stored} = \int_{\lambda_1}^{\lambda_2} i(\lambda).d\lambda \tag{2}$$

$$Energy(W) + Coenergy(W') = i.\lambda \tag{3}$$

$$W(\lambda, x)_{energy} = \frac{1}{2}.\frac{\lambda^2}{L(x)} \tag{4}$$

$$W'(i, x)_{coenergy} = \frac{1}{2}.L(x).i^2 \tag{5}$$

$$W'_{stored}(i_{1,......}i_j, x)_{coenergy} = \frac{1}{2}.\sum_{p=1}^{Nc}\sum_{q=1}^{Nc} L_{pq}.i_p.i_q \tag{6}$$

Equations 4 and 5 are general equations for energy and co-energy in the magnetostatic system. In equation 6, the electrical input count is N_c, and the position is represented by x. It is presumed that this co-energy is a part of a magnetic system with no loss. Outside the coupling field, losses are taken into account. (Liu et al., 2016). Self and bilateral inductances equation 7 can be calculated by obtaining the derivative of the co-energy related to any specific current from equation 6.

$$\frac{\partial W'f}{\partial i_p} = \sum_{q=1}^{Nc} L_{pq}.i_q = \lambda_{pt} \tag{7}$$

where by considering the approximate value of equation 7 with respect to a different currency, we can determine that λ_{pt} is the overall flux connecting the p^{th} core winding, which is created through all circuit currents. As a result, equation 8 gives the flux linkage between circuits p and q, and the self-inductance is recognized when p and q are equivalent.

$$\frac{\partial^2 W'f}{\partial i_p.\partial i_q} = L_{pq} = \frac{\partial \lambda_{pt}}{\partial i_q} \tag{8}$$

The FL approach can also be used to determine this mutual inductance. The rates of flux-linkage change with respect to currents in the situation of a linearized machine, where apparent inductances can be utilized, are constant and similar to the internal and bilateral inductances that are equation 9;

$$\frac{\partial \lambda_{pt}}{\partial i_q} = L_{pq} = L_{qp} = \frac{\lambda_p}{i_q} \tag{9}$$

where λ_p is the current flowing through winding i_q and p is the flux connecting windings p and q. This current alone generates the flux p. Equations 8 and 9 provide two techniques for calculating inductance that can be applied to magnetic fields that have been calculated numerically. The FL approach provides a simple procedure for equation 9. A non-linear magneto static numerical solution can be computed after all of the system's currents are known. From the B-H feature, it is possible to determine the conductivity of each component once this solution has been obtained equation 10.

$$\mu = \frac{B}{H} \tag{10}$$

It preserved in the grid of finite elements. The magnetic flux connections in overall the power transformer core windings owing to this current are acquired by uptake in the p^{th} winding. Therefore, equation 9 can be used to determine the internal and bilateral inductances connected to the p^{th} winding.

The winding vector notion, which attributes the fractional number of turns to nodes, allows for the efficient calculation of flow connections (Jia et al., 2022). Hence, only linear solutions are needed once the non-linear method has been discovered and each element's permeability has been locked. With just one more solution, all the inductances associated with the p^{th} winding may be calculated. The operational point's saturated circumstances under examination are represented by the values of inductance that were derived by substituting the saturated device with comparable equipment that includes a "sequential" feature through the equilibrium point. The inductance values for this analogous machine are correct, however, they need to be changed if the power transformer core deviates from its operational point. The graphs of variation of the irregular magnetization of the flux properties in the power transformer core depending on the field voltage are shown in Figure 1.

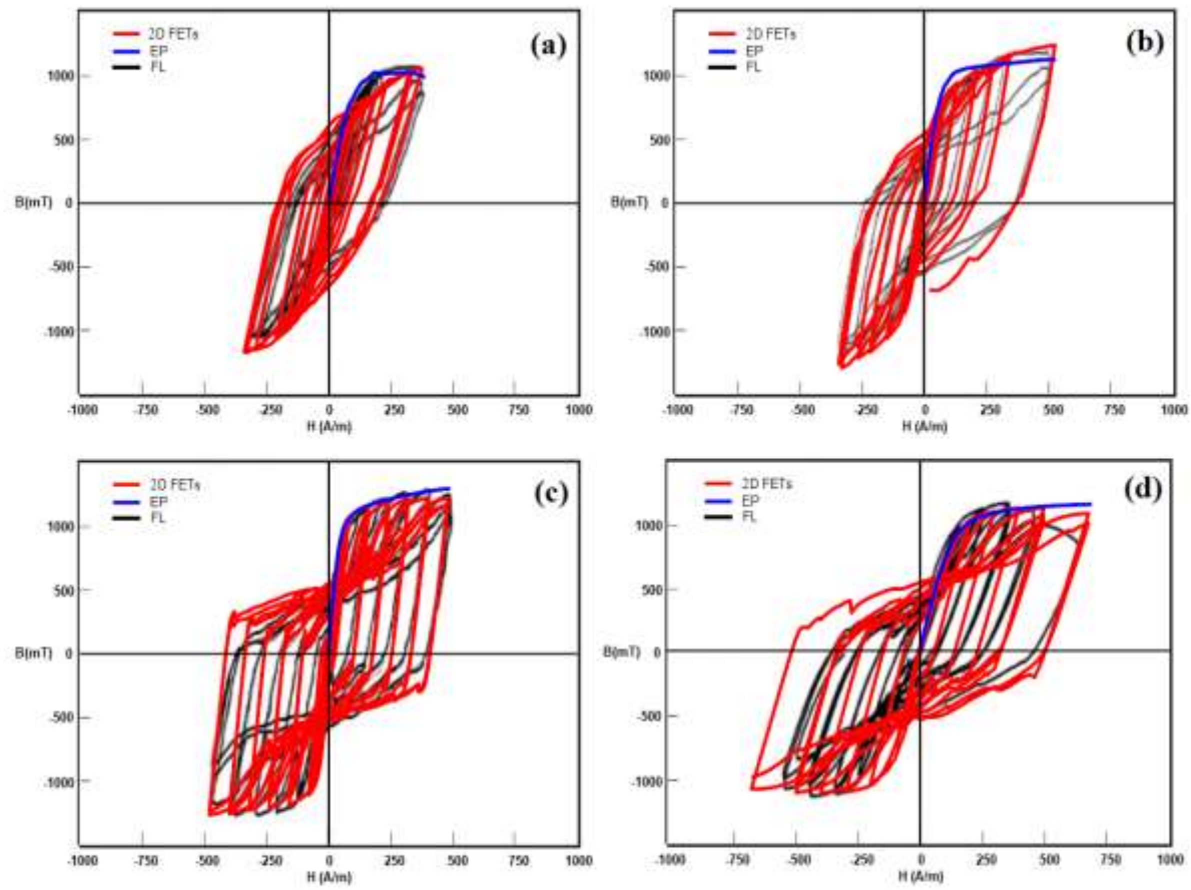

Figure 1. Field variation of uneven magnetic flux density in power transformer core windings, (a) for 144 equidistant air gap segments of the core settings, (b) for 288 equidistant air gap segments of the core settings, (c) for 864 equidistant air gap segments of the core settings, (d) for 1728 equidistant air gap segments of the core settings.

$$L_{pq} = \frac{\partial^2 W' f}{\partial i_p . \partial i_q} \approx \frac{\left[W' f(i_p + \Delta i_p, i_q + \Delta i_q) - W' f(i_p - \Delta i_p, i_q + \Delta i_q) - W' f(i_p + \Delta i_p, i_q - \Delta i_q) + W' f(i_p - \Delta i_p, i_q - \Delta i_q) \right]}{(4.\Delta i_p \Delta i_q)} \tag{11}$$

The FL strategy is an equivalent to the EP technique equation 11, which is connected to equation 8. However, once the FL magnetic solution has been identified this method needs more linear solutions. This may be observed from the approximate solution of equation 8 using finite differences;

This provides values for the mutual inductance ($p \neq q$). In equation 12, the self-inductance is specified.

$$L_{pp} = \frac{\partial^2 W' f}{\partial i_p . \partial i_p} \approx \frac{\left[W' f(i_p - \Delta i_p) - 2W' f + W' f(i_p + \Delta i_p) \right]}{(\Delta i_p)^2} \tag{12}$$

In equation 12, If all of the currents are present, the co-energy is *W'f*, and it is at the desired value, but with a partial positive shift in the p^{th} current is $W'f\ (i_p + \Delta i_p)$. All of the "perturbed" co-energies in equations 11 and 12 have the same interpretations. Since the FE system structure does not shift and also its reverse has already been established, only reverse replacements are necessary to calculate these perturbed co-energies. Keep in mind that the FL approach is equally applicable to this statement.

Due to the numerous solutions or back-substitutions necessary for their evaluation, it can be observed that equations 11 and 12 are awkward. For instance, four sequential approaches are necessary, three more than using the FL technique, to calculate the eddy current between the p^{th} and q^{th} windings. The flux-linkage strategy also offers a single sequential solution for the device winding under investigation and any associated bilateral inductances. Additionally, the post-processing of partial differential equation quantitative information ought to be considered to avoid evaluating variations between quantities of similar magnitude in order to prevent shaped faults, which is a disadvantage of the EP technique. When the necessary current increments are given to the EP approach, the numerical computation of the power transformer's core and magnetic area winding apparent inductances clearly demonstrates that the two methods are numerically equal.

The determination of apparent inductances in the field at a steady state of a power transformer winding using the EP method. The machine's real winding distribution served as a proxy for power transformer windings, and while calculating inductance values, it was necessary to account for the variance in inductance in relation to the winding design position. Utilizing 144 increments over 360 electrical degrees, inductance samples were collected. The self-inductance of a single phase, the leakage current between the magnetic and one phase, as well as the self-inductance of the primary coil, are all factors in the computation of the device inductance profiles. All in all, this means that the inductance computation process required 1728 linear solutions, but the FL technique would have just needed 288 solutions. It is obvious that, in terms of computing expenses, the FL technique is preferable.

2.2. Method for Calculating Differential Inductance Losses Numerically

A modified definition of inductance is required if the power transformer core cannot be substituted with an equivalent one that has apparent inductances. When apparent values are invalid, differential inductance is frequently used. In this case, the p^{th} winding's flux change rate in relation to the q^{th} current is no longer in effect. This changing rate was referred to as "gradual" inductance in the method. This is undesirable since the additional inductance is connected to minor signal changes around a specialist area, in which case magnetic materials take a different path than the regular B-H curve and instead superimpose incremental loops on the normal B-H profile. Since the inductance described by the gradient of the non-linear curve is better described by the label differential, it is used in this application. Replace the permeability definition in equation 10 with equation 13;

$$\mu = \frac{\partial B}{\partial H} \tag{13}$$

which, following the discovery of the power transformer core's quasi-solution, is derived from the standard B-H curve. Thus, for the operating situation and the calculation of difference inductances, values of "differential" leakage, are defined as equation 14;

$$L_{pq} = \frac{\partial \lambda_{pt}}{\partial i_q} \tag{14}$$

is now possible to calculate the differential inductance by suspending the difference admittance in the mathematical model and injecting individual currents into the windings;

$$L_{pq} = \frac{\lambda_p \left| \frac{\partial B}{\partial H} \right.}{i_q} \tag{15}$$

where it is presumptively supposed that the system is linearized close to its operational point. Equation 15 is accurate because equation 13 resembles the differential of the flux-linkage in relation to the current. Equation 10 is replaced by equation 13 for the basic mathematical calculation of the "perturbed" energy, while equations 11 and 12 are still applicable for the computation of "difference" values. The following examples make it simple to demonstrate this claim. The differentiated electromagnetic co-energy of a dynamic function with N_c electricity sources and N_m physical outputs is given by equation 16;

$$dW'f = \sum_{p=1}^{Nc} \lambda_{pt}.di_p + \sum_{r=1}^{Nm} T_r.d\theta_r \tag{16}$$

where, T_r is the power transformer core's measured r^{th} electromagnetic torque. It is also possible to write the entire differential of co-energy as equation 17;

$$dW'f = \sum_{p=1}^{Nc} \frac{\partial W'f}{\partial i_p}.di_p + \sum_{r=1}^{Nm} \frac{\partial W'f}{\partial \theta_r}.d\theta_r \tag{17}$$

Hence, by equating 16 and 17, the equation 18;

$$\lambda_{pt} = \frac{\partial W'f}{\partial i_p} \tag{18}$$

It provides the necessary outcome after differentiation with regard to the q^{th} current equation 19;

$$\frac{\partial^2 W'f}{\partial i_q \partial i_p} = \frac{\partial \lambda_{pt}}{\partial i_q} = L_{pq} \tag{19}$$

Calculating differential inductance quantities has the same limitations as calculating apparent inductance numerically using "perturbed" co-energies.

It ought to be noted that the system's stored energy rather than the co-energy is utilized. This is obviously erroneous when determining differential inductances, but it is correct when calculating apparent inductances. As a result, it is clear that both procedures provide identical inductance values. Since both methods are derived from the same physical foundation, this is not surprising. However, since it avoids numerical differentiation and just requires a limited number of sequential values, the FL technique provides an effective and reliable way to determine inductance values in 2D. The calculation of differential inductances for a power transformer core is described. The "energy perturbation method" was used for this calculation. To perform this calculation, the flux-linkage approach might have needed a lot fewer alternatives.

3. Modeling and Numerical Example of Power Transformer Core with Finite Element Methods

Calculating the time variation of the apparent inductance values of a power transformer core operating under different operating conditions demonstrates the numerical equality of the FL and EP approaches. Due to the significant air gap they imply, apparent values are suitable for solid-power transformer cores. The finite element model as well as the transient conditions of the machine under consideration are fully described. Nevertheless, the machine operating conditions are briefly described here. The core is initially working under-excited (on-load) and connected to the main power system. A three-phase-to-earth fault is applied to the high-voltage connectors of the power transformer core. The fault duration is seven cycles.

The equipment is then reconnected to the main system after the problem has been fixed. A stable condition is achieved after fault clearance. For the fault period, inductance values are computed. The field winding and the fictional *d* and *q* axis cyclic distributed windings, which are fixed to the core stationary frame, are included in the self-inductances that were calculated. The effective turns on these *d* and *q*-axis windings match the number of real turns on each phase coil. Consequently, two windings have been used in place of the actual three-phase winding, and their mathematical representations take the form of two winding vectors, the entries of which are as follows equation 20;

$$N_{di} = \frac{4}{\pi} N_{eff} \frac{l_i.\sin\Theta i}{\sum_{j=1}^{n} \left| l_j.\sin\Theta j \right|}, \quad N_{qi} = \frac{4}{\pi} N_{eff} \frac{l_i.\cos\Theta i}{\sum_{j=1}^{n} \left| l_j.\cos\Theta j \right|} \tag{20}$$

where l_i is the length assigned to node *i* and Θi denotes the angle this node makes with the *d* axis. N_{eff}, which accounts for winding factors, is the quantity of evenly spaced air gap effective turns. The total is computed over the nodes that correspond to the power transformer core winding. To determine core inductances in the power transformer winding current frame, the magnetic state of the power transformer core at every sampling interval is used. The three-phase coordinate system is used to build the 2D-finite element analysis.

All of the power transformer winding eddy currents must be understood in order to use the EP approach. The transient FE solution provides these currents. Finding the power transformer core's *d* and *q*-axis current characteristics for every duration level is important so as to compute the d-q-axis inductances. Applying all of the power transformer core currents together with the armature's axis currents to the FE grid, where the reluctivity is determined from the FE transient solution, yields the co-energy at the operating point. Utilizing current increments that are inversely proportional to the predicted power transformer core instantaneous currents at each time step, perturbed co-energies are created. On the other hand, the FL approach necessitates injecting an arbitrary current into the relevant winding in order to get inductance values. The FE transient solution also allows for the determination of element reluctivity for the linear solution. Figure 2 displays the time-dependent self-inductance variation graph. Figure 2 compares the power transformer core winding apparent inductances calculated from the FL and EP methods.

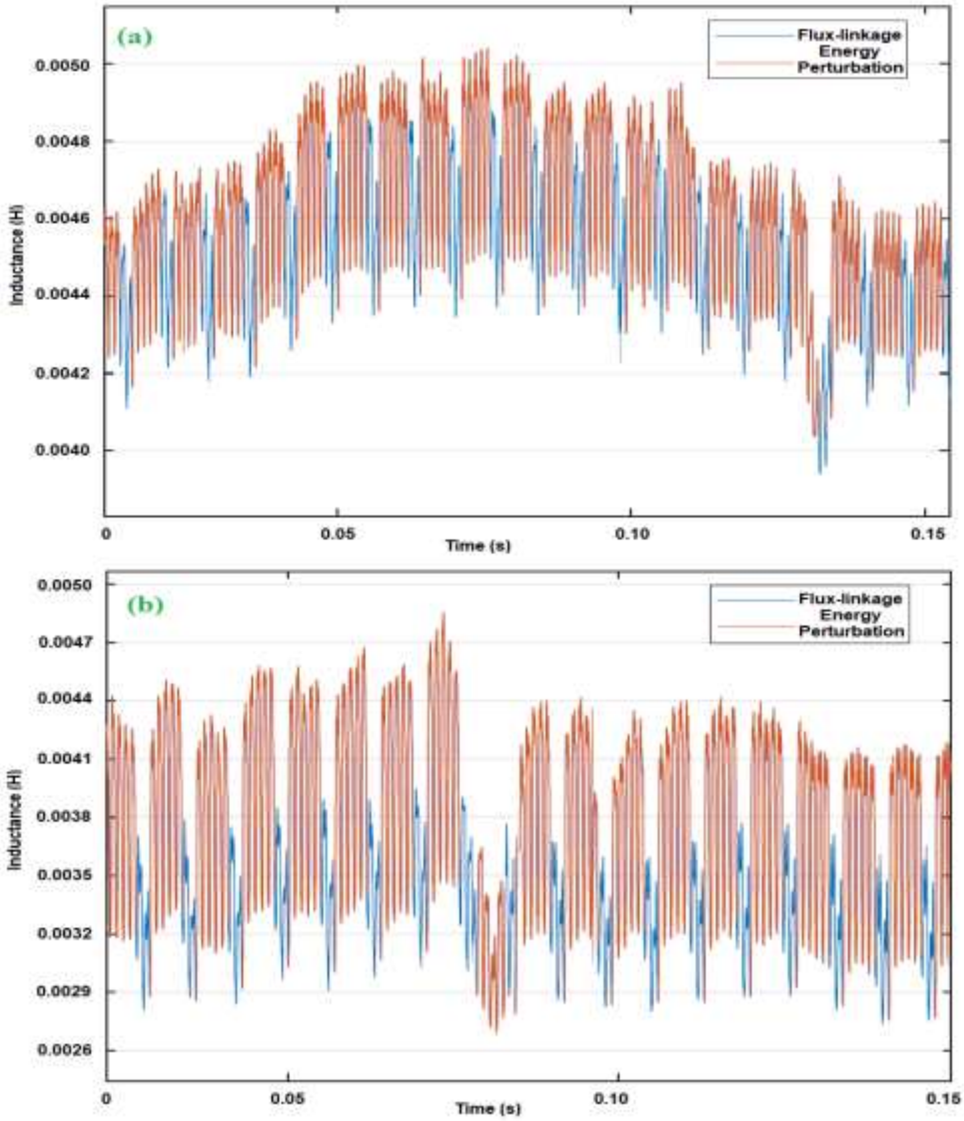

Figure 2. Time-dependent self-inductance variation in power transformer core windings (a) for d-axis, (b) for q-axis.

It has been shown that both methods produce values that are essentially identical. The *d* and *q* axis self-inductances determined using the EP approach, however, exhibit spikes. They manifest while the regular currents are still several orders of magnitude less than the modestly sized *d* or *q*-axis currents. The extremely small difference between the perturbed energy results in numerical issues. It should be noted that this issue can be solved by selecting larger current increments to increase the disparity between energies.

The field power transformer core winding self-inductance variation graph is shown in Figure 3. The power transformer core bilateral inductance between both the field and the *d*-axis winding variation graph is shown in Figure 4.

This challenge is not present when calculating the self and bilateral inductance of the field winding since the field current never gets close to null during the fault current time. The four inductance values presented here were obtained using the EP approach, which needed ten linear replacements or backward substitutions for each time unit. The FL approach simply needed three step. The EP approach will require a significantly greater number of calculations if there are more power transformer core windings.

4. Conclusion

In regards to computational costs and numerical instabilities, two approaches for calculating the inductance of practically achievable power transformer core windings were compared. They provide comparable inductance values for an abnormally performing power transformer. This is hardly remarkable because both approaches are predicated on the same ideas. The EP approach is computationally expensive, though, and if increment currents are not properly selected, numerical issues may arise. Therefore, when using 2D-FE solutions, the FL approach must be chosen as the optimal method for calculating the inductances of electricity transformer core windings since it offers a great deal of simplicity and lower computing costs.

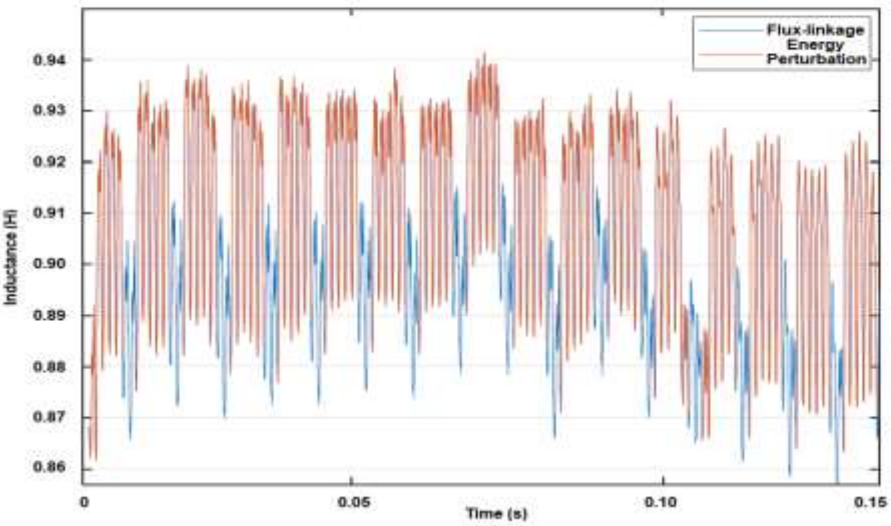

Figure 3. The field power transformer core winding self-inductance.

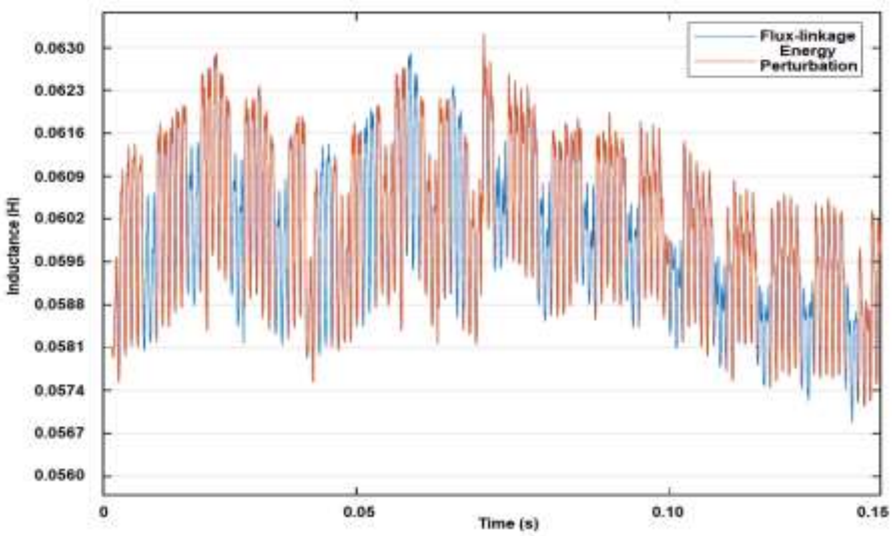

Figure 4. Power transformer core bilateral inductance between both the field and the d-axis windings.

Author Contributions

The percentage of the author contributions is present below. The author reviewed and approved final version of the manuscript.

	N.P.
C	100
D	100
S	100
DCP	100
DAI	100
L	100
W	100
CR	100
SR	100
PM	100
FA	100

C=Concept, D= design, S= supervision, DCP= data collection and/or processing, DAI= data analysis and/or interpretation, L= literature search, W= writing, CR= critical review, SR= submission and revision, PM= project management, FA= funding acquisition.

Conflict of Interest

The author declared that there is no conflict of interest.

References

Awadallah SKE, Milanović JV, Jarman PN. 2014. The influence of modeling transformer age related failures on system reliability. IEEE Transact Power Syst, 30(2): 970-979. doi:10.1109/TPWRS.2014.2331103.

Božidar FG, Franc B, Uglešić I, Pavić I, Keitoue S, Murat I, Ivanković I. 2017. Monitoring of transient overvoltages on the power transformers and shunt reactors–field experience in the Croatian power transmission system. Procedia Eng, 202: 29-42. doi:10.1016/j.proeng.2017.09.692.

Delghavi MB, Yazdani A, Alizadeh A. 2021. Iterative learning control of dispatchable grid-connected distributed energy resources for compensation of grid current harmonic distortions. Int J Electrical Power Energy Syst, 131: 107064. doi:10.1016/j.ijepes.2021.107064.

Ding X, Ning W. 2012. Analysis of the dry-type transformer temperature field based on fluid-solid coupling. Second International Conference on Instrumentation, Measurement, Computer, Communication and Control, December 8-10, 2012, Harbin City, Heilongjiang, China, pp: 520-523.

Emiroglu S, Uyaroglu Y, Gumus TE. 2021. Recursive backstepping control of ferroresonant chaotic oscillations consisting between grading capacitor with nonlinear inductance of voltage transformer. European Physical J, 230: 1829-1837. doi:10.1140/epjs/s11734-021-00150-9.

Ertl M, Landes H. 2007. Investigation of load noise generation of large power transformer by means of coupled 3D FEM analysis. Int J Comput Math Electr Electron Eng, 26(3): 788-799. doi:10.1108/03321640710751226.

Fornasiero E, Bianchi N, Soong WL. 2014. Analysis of torque versus current capability of reluctance and interior pm machines under limited current and flux-linkage operation. IEEE Energy Conversion Congress and Exposition (ECCE), September 14-18, 2014, Pittsburgh, Pennsylvania, US, pp: 4162-4169. doi:10.1109/ECCE.2014.6953968.

Hashemnia N, Abu-Siada A, Islam S. 2015. Improved power transformer winding fault detection using FRA diagnostics–part 2: radial deformation simulation, IEEE Transact Dielectrics Electr Insulation, 22(1): 564-570. doi:10.1109/TDEI.2014.004592.

He JH. 2003. Homotopy perturbation method: a new nonlinear analytical technique. Appl Math Comput, 135(1): 73-79. doi:10.1016/S0096-3003(01)00312-5.

Jia X, Lin M, Su S, Wang Q, Yang J. 2022. Numerical study on temperature rise and mechanical properties of winding in oil-immersed transformer. Energy, 239(A): 121788. doi:10.1016/j.energy.2021.121788.

Johnson A, Wang X, Xue M, Kong F, Zhao G, Wang Y, Thomas KW, Brewster KA, Gao J. 2014. Multiscale characteristics and evolution of perturbations for warm season convection-allowing precipitation forecasts: Dependence on background flow and method of perturbation. Monthly Weather Rev, 142(3): 1053-1073. doi:10.1175/MWR-D-13-00204.1.

Kunicki M, Borucki S, Zmarzły D, Frymus J. 2020. Data acquisition system for on-line temperature monitoring in power transformers. Measurement, 161: 107909. doi:10.1016/j.measurement.2020.107909.

Kwon YW, Bang H. 2018. The finite element method using MATLAB, 2nd Edition. CRC Press, London, UK, pp: 622.

Lee M, Abdullah HA, Jofriet JC, Patel D. 2010. Thermal modeling of disc-type winding for ventilated dry-type transformers. Electr Power Syst Res, 80(1): 121-129. doi:10.1016/j.epsr.2009.08.007.

Liu C, Ruan J, Wen W, Gong R, Liao C. 2016. Temperature rise of a dry-type transformer with quasi-3D coupled-field method. IET Electric Power Appl, 10(7): 598-603. doi:10.1049/iet-epa.2015.0491.

Mariprasath T, Ravindaran M. 2022. An experimental study of partial discharge analysis on environmental friendly insulating oil as alternate insulating material for transformer. Sādhanā, 47: 204. doi:10.1007/s12046-022-01946-8.

Mejia-Barron A, Valtierra-Rodriguez M, Granados-Lieberman D, Olivares-Galvan JC, Escarela-Perez R. 2018. The application of EMD-based methods for diagnosis of winding faults in a transformer using transient and steady state currents. Measurement, 117: 371-379. doi:10.1016/j.measurement.2017.12.003.

Metwally IA. 2011. Failures, monitoring and new trends of power transformers. IEEE Potentials, 30(3): 36-43. doi:10.1109/MPOT.2011.940233.

Oliveira LMR, Cardoso AJM. 2014. Leakage inductances calculation for power transformers interturn fault studies. IEEE Transact Power Deliv, 30(3): 1213-1220. doi:10.1109/TPWRD.2014.2371877.

Oliveira MO, Ferreira GD, García FH, Bretas AS, Perrone OE, Reversat JH. 2012. Adaptive differential protection for power transformer based on transient signal analysis. IEEE Power and Energy Society General Meeting, July 22-26, 2012, San Diego, CA, US, pp: 1-7. doi:10.1109/PESGM.2012.6344824.

Pamuk N. 2017. Identification of critical values based on natural ester oils as potential insulating liquid for high voltage power transformers. J Polytech, 20(4): 869-877. doi:10.2339/politeknik.369050.

Shadab S, Revati G, Wagh SR, Singh NM. 2023. Finite-time parameter estimation for an online monitoring of transformer: A system identification perspective. Int J Elect Power Energy Syst, 145: 108639. doi:10.1016/j.ijepes.2022.108639.

Shirakawa T, Yamasaki G, Umetani K, Hiraki E. 2016. Copper loss analysis based on extremum co-energy principle for high frequency forward transformers with parallel-connected windings. IECON 2016 - 42nd Annual Conference of the IEEE Industrial Electronics Society, October 23-26, 2016, Florence, Italy, pp: 1099-1105.